Comparative performance of fluorite-structured materials for nanosupercapacitor applications

Grégoire Magagnin, Jordan Bouaziz, Martine Le Berre, Sara Gonzalez, Damien Deleruyelle, Bertrand Vilquin

Comparative Performance of Fluorite-Structured Materials for Nanosupercapacitor Applications

Grégoire Magagnin,[1] Jordan Bouaziz,[1] Martine Le Berre,[2] Sara Gonzalez,[3] Damien Del eruyelle,[2] and Bertrand Vilquin[1]

[1)] *Ecole Centrale de Lyon, INSA Lyon, CNRS, Universite Claude Bernard Lyon 1, CPE Lyon, INL, UMR5270, 69130 Ecully, France*

[2)] *INSA Lyon, Ecole Centrale de Lyon, CNRS, Universite Claude Bernard Lyon 1, CPE Lyon, INL, UMR5270, 69621 Villeurbanne, France*

[3)] *CNRS, INSA Lyon, Ecole Centrale de Lyon, Universite Claude Bernard Lyon 1, CPE Lyon, INL, UMR5270, 69621 Villeurbanne, France*

(Dated: July 8, 2024)

Over the last fifteen years, ferroelectric and antiferroelectric ultra thin films based on fluorite-structured materials have drawn significant attention for a wide variety of applications requiring high integration density. Antiferroelectric ZrO_2, in particular, holds significant promise for nanosupercapacitors, owing to its potential for high energy storage density (ESD) and high efficiency (η). This work assesses the potential of high-performance $Hf_{1-x}Zr_xO_2$ thin films encapsulated by TiN electrodes that show linear dielectric (LD), ferroelectric (FE), and antiferroelectric (AFE) behavior. A wake-up (WU) effect is observed for AFE ZrO_2, a phenomenon barely reported for pure zirconium oxide and AFE materials in general, correlated to the disappearance of the pinched hysteresis loop commonly observed for Zr-doped HfO_2 thin films. ESD and η are compared for FE, AFE, and LD samples at the same electrical field (3.5 MV/cm). As expected, ESD is higher for the FE sample (95 J/cm^3), but η is ridiculously small ($\approx$ 55 %), because of the opening of the FE hysteresis curve inducing high loss. Conversely, LD samples exhibit the highest efficiency (nearly 100 %), at the expense of a lower ESD. AFE ZrO_2 thin film strikes a balance between FE and LD behavior, showing reduced losses compared to the FE sample but an ESD as high as 52 J/cm^3 at 3.5 MV/cm. This value can be further increased up to 84 J/cm^3 at a higher electrical field (4.0 MV/cm), with an η of 75 %, among the highest values reported for fluorite-structured materials, offering promising perspectives for future optimization.

I. INTRODUCTION

Immediate remedies are essential to address the challenges posed by the exponential increase of energy consumption. Specifically, pivotal technologies related to the fourth industrial revolution—such as the Internet of Things and Big Data—are witnessing an exponential surge in energy consumption linked to the storage, processing, and transmission of digital information[1]. Harnessing the potential of ferroelectric (FE) and antiferroelectric (AFE) materials compatible with complementary metal–oxide–semiconductor (CMOS) technology is a compelling strategy for the creation of energy-efficient electronic devices more specifically for energy conversion applications[2].

The term "Fluorite structure" denotes a prevalent pattern observed in compounds represented by the formula MX_2. In this arrangement, the X ions are situated in the eight tetrahedral interstitial sites, while the M ions occupy the regular sites within a face-centered cubic structure. This structural configuration is commonly observed in various compounds, notably the mineral fluorite (CaF_2) which gave its name to the structure. Typical fluorite-structured ferroelectrics and antiferroelectrics are respectively doped hafnium oxide (HfO_2) and zirconium oxide (ZrO_2). HfO_2 has been introduced since 2007 by Intel as a high-k (high dielectric constant) in the gate stack of MOS transistors (metal oxide semiconductor)[3] while ZrO_2 is also widely used to fabricate DRAM cells[4]. In 2011, a ferroelectric phase in Si-doped HfO_2 was first reported[5,6], followed by the discovery of ferroelectricity in a solid solution of $Hf_{0.5}Zr_{0.5}O_2$ (HZO) the same year[7], paving the way for the re-introduction of ferroelectric materials in the existing CMOS technology.

At atmosphere pressure, bulk HfO_2 and ZrO_2 have centrosymmetric non-polar crystal structures[8]. However, under certain conditions of TiN encapsulation, doping and/or film stress, it is possible to stabilize a meta-stable orthorhombic phase, which gives rise to ferroelectricity (FE) in HfO_2 and in HfO_2-ZrO_2 thin film solid solutions[9]. Contrary to antiferroelectricity originating from anti-parallel dipole moments, the origin of the functional AFE properties in ZrO_2 is attributed to an electric field induced non-polar to polar phase transition[10]. The field-induced structural phase transition in ZrO_2 is attributed to a reversible non-polar tetragonal phase to a polar orthorhombic phase[11], ensuing in a double hysteresis polarization loop (PE loop) with an applied electric field[12].

FE and AFE nanosupercapacitors can be used for solid-state electrostatic energy storage[13]

where high energy storage performances has been reported in ferroelectric HfO_2 or ZrO_2 films[14–16]. The field-induced transitions observed in AFE ZrO_2 hold promise for energy storage applications. However, several physical parameters from the fluorite films can limit the energy storage performances. Ferroelectric thin films exhibit a "wake-up" (WU) effect, which corresponds to an increase of the remnant polarization with cycling. This effect depends on the amplitude and frequency of the cyclic applied voltage stress[17]. Another limiting factor is the film thickness scaling. Fluorite films have limited energy storage scaling properties due to the increase of the monoclinic phase proportion at large thicknesses[18].

Ferroelectrics (FE) excel in achieving high polarization, leading to high energy storage density (ESD). However, they have rather low efficiency, while linear dielectrics (LD) demonstrate remarkable efficiency, but low polarization[19]. In the context of prior research, it becomes evident that antiferroelectrics (AFE) offer an optimal balance, offering superior characteristics by combining elevated ESD and higher efficiency. Surprisingly, the exploration of these distinct attributes within the same material, thickness, and capacitor structures has been notably limited. In this context, this work aims at addressing this gap, employing ZrO_2 and HZO as prototype materials for a comprehensive investigation. This study proposes a performance assessment and comparison between AFE, FE and LD fluorites for nanosupercapacitor applications. Fluorite thin films were grown with the same chemical composition but with different deposition techniques and parameters, leading to different nanosupercapacitor electrical properties, from LD to FE and AFE. AFE fluorite thin films exhibit beyond state-of-the-art energy storage capabilities.

II. MATERIALS AND METHODS

Capacitors were fabricated on p-doped Si (001) substrates and follow the stack Pt / TiN / oxide / TiN / Si. Details of the deposition processes for oxides are summarized in table I. Sputtering is performed via AC450 magnetron sputtering chamber from Alliance Concept, while Plasma-Enhanced Atomic Layer Deposition (PEALD) is carried by a Fiji F200 apparatus from Ultratech. The first step of ZrO_2 PEALD deposition consists in the application of an O_2 plasma on the TiN bottom electrode at 300 W, before opening the valve of the TDMA-Zr precursor. Alternation of a complex sequence, notably including the TDMA-Zr valve opening and the dioxygen plasma is then performed to grow the AFE

Oxide	HZO(LD)	HZO(FE)	ZrO_2(LD)	ZrO_2(AFE)
Deposition Technic	Reactive sputtering	Non-Reactive Sputtering	Reactive Sputtering	PEALD
Working Pressure (mbar)	5×10^{-3}	5×10^{-2}	5×10^{-3}	5×10^{-1}
Target or Precursors	Hf/Zr	HfO_2/ZrO_2	Zr	TDMA-Zr
Deposition Temperature	Room Temperature			200 °C
RTA	450 °C - 30 s - N_2 atmosphere			600 °C - 30 s - N_2 atmosphere
Thickness (nm)	9.1	13.0	8.5	10.3

Table I. Growth conditions of the oxide thin films. Electrical properties of the films are shown in figure 1 and given in the brackets.

ZrO_2 thin film. Sputtering is performed for TiN and Pt using a metallic target of Ti and Pt. Pt/TiN top electrodes are obtained after a photolithography and lift-off process. Rapid thermal annealing (RTA) was then performed for all samples. Samples where then investigated by means of physical and electrical characterization.

Glancing Incidence X-ray Diffraction (GIXRD) was performed on a Smartlab Rigaku diffractometer using a 9 kW copper rotating anode, a parabolic multi layer mirror for parallel beam setting, Ni filter for CuK_α radiation selection, 0.114° aperture parallel slit analyser, and a 0D scintillating counter. The thickness of all thin films was measured by X-Ray Reflectivity (XRR) with the same instrument.

Electrical characterization was carried out on 50 µm and 20 µm diameter capacitors using a probe station in a Faraday cage and a setup composed of a Keithley 4200SCS equipped with PMU. Endurance tests were performed using a custom program interfaced with the Keithley. The cycling sequence consists in bipolar voltage square pulses (commonly called set/reset sequence) until breakdown at 3.5 V to 4.5 V depending on the film thickness with 20 µs pulse duration. Polarization as a function of electric field (P-E) curves are established from the measurement sequence consisting 3 triangle pulses (DHM : Dynamic Hysteresis Measurement) with a 60 µs rise time. The first voltage pulse poles the polarization in a given pre-set direction, while the two other pulses measures the current response. The pulse amplitude is set to obtain a 3.5 MV/cm electrical field for each samples, and for all figures, except figure 5, where a maximum electrical field of 4.0 MV/cm is applied in order to maximize the ESD of the AFE ZrO_2.

III. RESULTS AND DISCUSSION

The field induced electrical properties of the fluorite thin film capacitors grown by sputtering and ALD were first examined. Fig 1 shows the electrical characteristics of the capacitors comparing FE and AFE samples with LD ones of the same chemical composition, at the same applied electric field of 3 MV/cm. On Figure 1, FE, AFE and LD properties of HZO and ZrO_2 are shown after 10^3 cycles. Polarization versus electrical field (solid curves) and current versus voltage (dashed curves) are systematically shown for each studied samples.

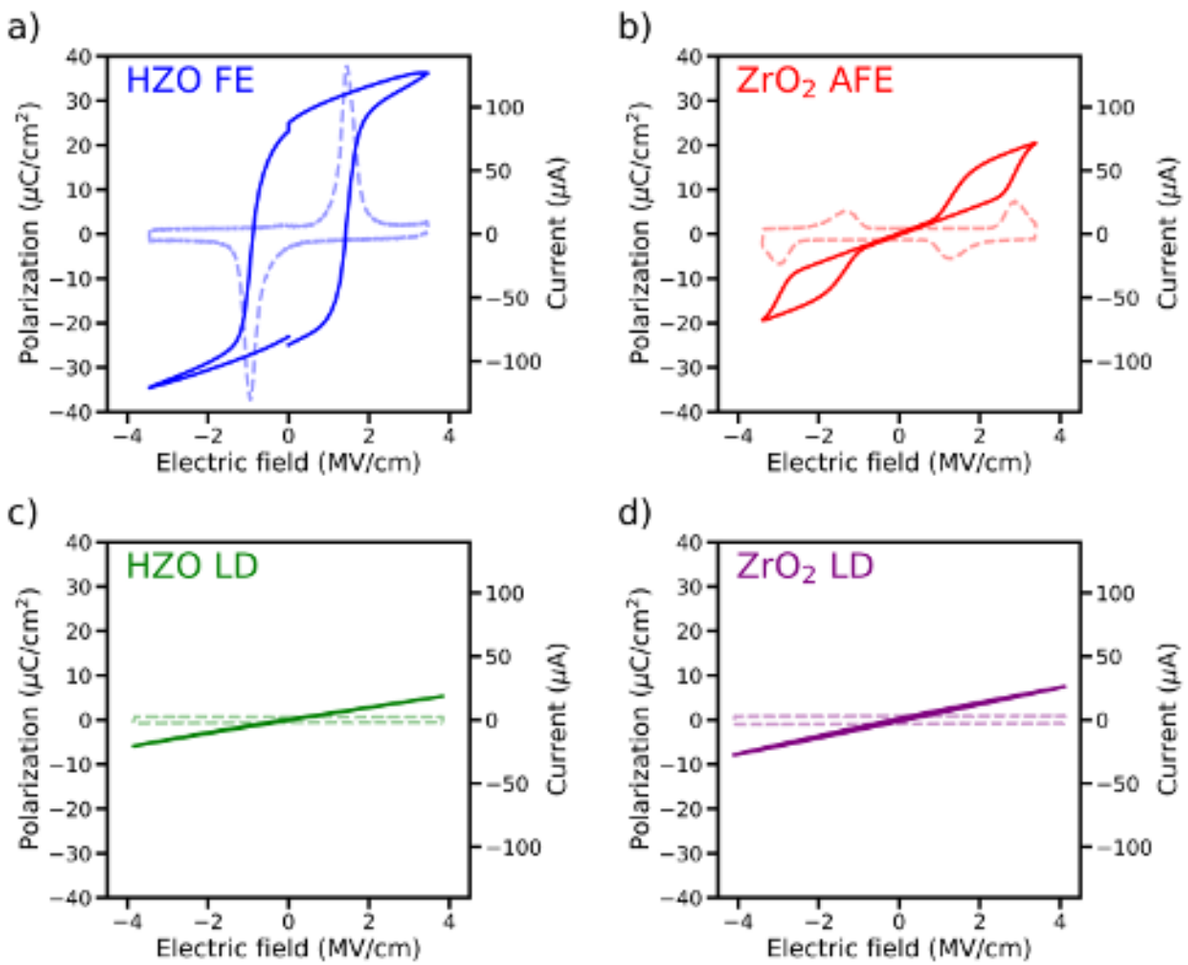

Figure 1. Polarization versus Electrical field (straight lines) and Current versus Voltage (dashed lines) after 10^3 cycles for a) a ferroelectric $Hf_{0.5}Zr_{0.5}O_2$ (FE HZO), b) an anti-ferroelectric ZrO_2 (AFE ZrO_2), c) a linear dielectric $Hf_{0.5}Zr_{0.5}O_2$ (LD HZO) and d) a linear dielectric ZrO_2 (LD ZrO_2).

For LD samples on Figure 1(c) and (d), as the dielectric capacitor is charging or discharging, the current is different from zero, leading to a non-zero electric displacement field for non-zero electric field. Therefore, a linear relationship between polarization and the applied electric field is expected. Due to leakage currents, the P-E loop is not totally closed and will lead to an efficiency of the energy storage close but less than 100 % (the theoretical value for a perfect LD).

For the FE HZO on Figure 1(a), after 10^3 cycles, two peaks can be observed: one at positive voltages and one at negative voltages. These peaks corresponds to polarization switching peaks, due to the FE nature of the film, attributed to the displacement of oxygen ions in HZO[20]. The remnant polarization of the FE HZO is 23 µC/cm^2 on the positive side and 24 µC/cm^2 on the negative side. The small asymmetry is attributed to the possible oxidation state of the top[21] or bottom[22] TiN electrode.

Finally, for the AFE ZrO_2 sample, a state-of-the-art curve is observed after 10^3 cycles. A threshold field of about 1.0 MV/cm can be seen between an LD to FE behavior, corresponding to the field induced phase transition assumed for ZrO_2[11,23]. A very sharp linear opening is present below 1.0 MV/cm followed by a narrow hysteresis loop above, with a saturation polarisation P_s as high as 20.5 µC/cm^2.

Structural characterization measurements are then conducted on each sample to elucidate the origin of the functional properties allowing for energy storage. Figure 2 shows the XRD scans for all FE, AFE and LD samples. The FE HZO sample exhibits a distinct orthorhombic/tetragonal (o/t) peak with (111) orientation for the o-phase and (101) orientation for the t-phase around a 2θ value of 30.5°. The non-centrosymmetric o-phase is typically considered the phase responsible for ferroelectricity. However, it also shows the presence of the monoclinic (m-) phase, which is centrosymmetric. The mixture of o/t phases is attributed to HZO, while only the (101)-oriented t-phase is attributed to ZrO_2 for the peak around 30.5°, considering current literature explanations[23,24].

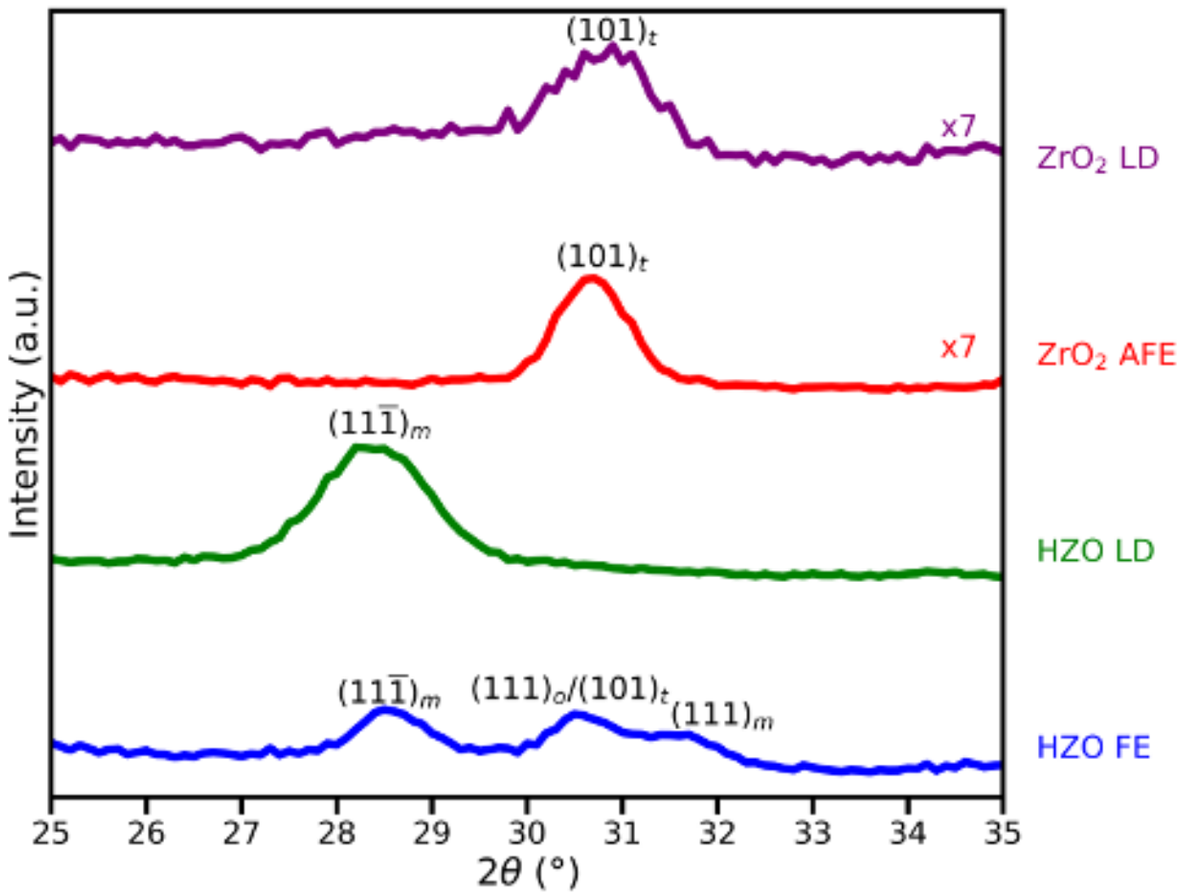

Figure 2. GIXRD scans of FE HZO (red curve), AFE ZrO_2 (blue curve), LD ZrO_2 (green curve), LD HZO (purple curve).

Properties of HZO thin films of (approximately 10 nm thick), synthesized via reactive magnetron sputtering from a Hf/Zr metallic target[22,25] on a TiN layer, were explored. GIXRD measurements revealed that, depending on the deposition working pressure in the chamber – low pressure (LP) (5×10^{-3} mbar) or high pressure (HP) (5×10^{-2} mbar) – the thin films were either monoclinic or amorphous after deposition. The ZrO_2 films grown by ALD[7] are amorphous after deposition. Amorphous samples exhibit the o/t peak after Rapid Thermal Annealing (RTA), while monoclinic samples remain in their monoclinic structure after RTA.

For the HfO_2/ZrO_2 ceramic target and the Zr metallic target used in this study (respectively non-reactive and reactive magnetron sputtering), regardless the pressure, the HZO and ZrO_2 thin films are amorphous after deposition. After RTA, films obtained at both

pressures exhibit the o/t peak, but only the HZO HP samples also show some monoclinic peaks, whereas LP samples only show the o/t peak (not shown in this paper). It was demonstrated that HZO LP samples are only tetragonal[26] while HP samples show a mixture of tetragonal and orthorhombic phase (in addition to the monoclinic phase for HP samples).

While all samples present the o/t peak in their GIXRD scans, their electrical behaviors are vastly different. Our observations tend to show that observing a peak around 30.5° is a necessary condition to have FE or AFE properties, but it is not a sufficient condition. For HZO samples, the FE signature is given by the presence of the $(111)_o$ peak, which is overlapping with the $(101)_t$ peak. Their respective contributions can only be evaluated by fitting the peaks. For ZrO_2 samples the $(101)_t$ peak is not enough to discriminate between LD and AFE. Structural measurements alone are generally insufficient to clearly identify the electrical nature of the thin films. Therefore, electrical characterizations in Figure 1 are needed to conclude about the electric nature of the HZO and ZrO_2 capacitors.

Endurance tests were also performed and a wake-up effect was observed. Historically, the first observation of a wake-up effect dates back to Sim et al.[27]. However, in Sim et al. article, the increase in P_r seems to be attributable to the increase in leakage current (fatigue phenomena) at increasing cycling counts. There is no evidence that this effect could be similar to that observed for HfO_2. In 2011, Wu et al.[28] continued the work of Sim et al. They coined, for the first time, the increase in Pr with the number of cycles as the "wake-up" effect. However, here again, this so-called "wake-up" effect can be attributed to the increase in leaks and phenomena of modification of space charge. In the same article, it is also noted that if the frequency decreases, P_r increases. In 2012, finally, Mueller et al.[29] released the first article discussing the "wake-up" effect on Si:HfO_2. They named this effect the wake-up effect in reference to the endurance test procedure carried out by Wu et al. and then spoke of a "wake-up procedure" and not a "wake-up effect." In 2013, Zhou et al.[17] were the first to truly study the wake-up (WU) effect and to name it as such. This time, the argument of increased leaks is no longer mentioned, although this is not conclusively proven in this article. Thanks to the electrical characterization PUND technique, it was already observed in previous works that the WU effect does not result from an increase in leakage currents[30]. Moreover, Zhou et al. observe that as the measurement frequency increases, Pr decreases, while it would increase at increasing pulse voltage amplitudes. It will be shown later that a WU effect is also present for AFE ZrO_2, a detailed observation of the wake up and endurance

properties of the analyzed films is present in the supplemental materials. This WU effect, although almost identical from the perspective of current shifts along cycling in FE HZO and AFE ZrO_2, cannot be defined as an increase of P_r.

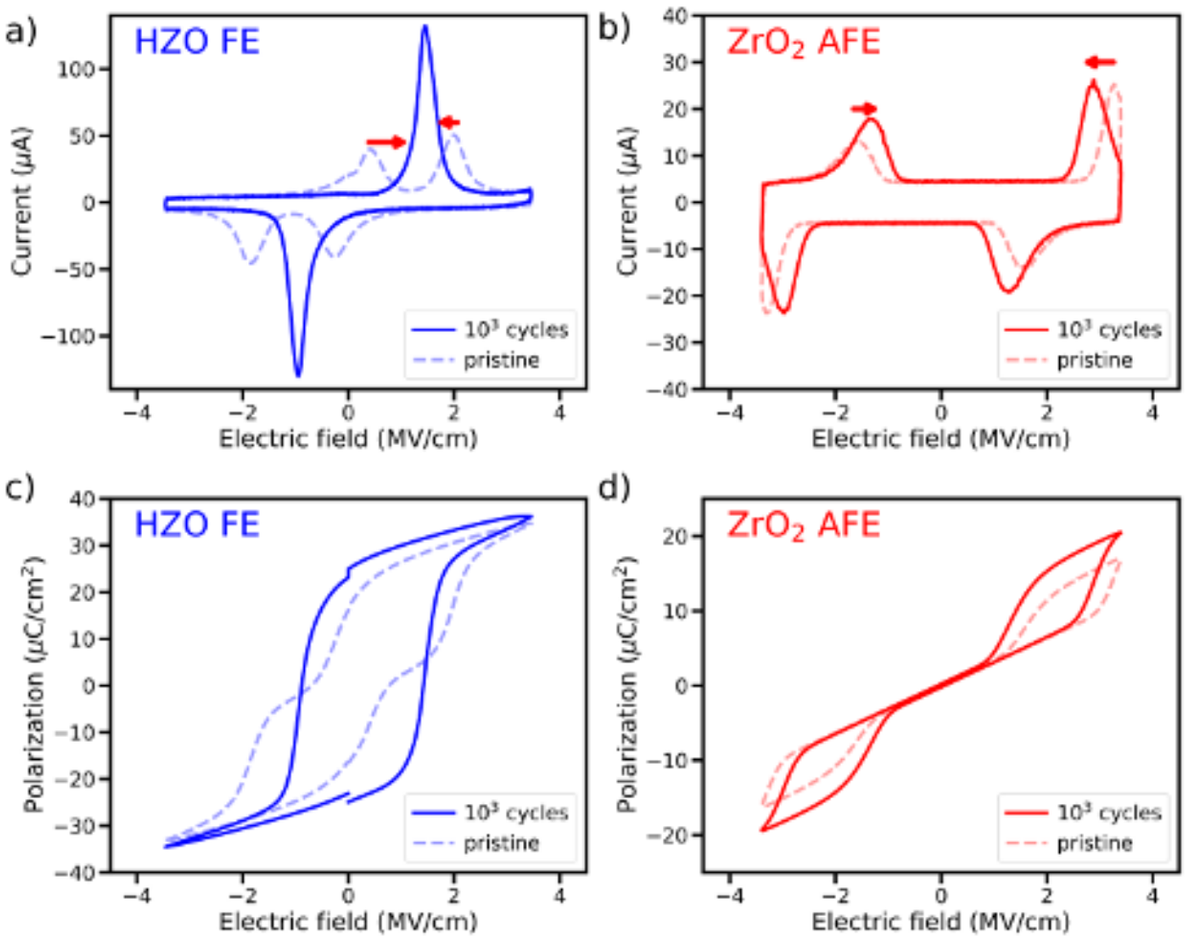

Figure 3. Current versus electric field measurements for pristine samples (dashed lines) and 10^3 cycles (straight lines) of (a) FE HZO (b) AFE ZrO_2 and their corresponding polarization versus electric field measurements of (c) FE HZO (d) AFE ZrO_2. The observed change in current between pristine and 10^3 cycled samples correspond to the wake-up effect (WU), resulting in the switching current peaks shift over the voltage axis highlighted by the red arrows.

Figure 3a) and b) depict current versus voltage (I-V) curves for FE HZO and AFE ZrO_2, respectively, whereas Figure 3c) and d) illustrate P-E loops for the same samples. Dashed lines represent the behavior of the samples in their pristine state, while solid lines indicate their behavior after 10^3 endurance cycles. At the pristine stage, FE HZO exhibits 4 switching

current peaks : one pair at positive voltages and another one at negative voltages (dashed lines Figure 3(a)). Along cycling, each pair would progressively merge (solid lines Figure 3(a)), leading to the hysteresis loop on Figure 1c) (solid lines). For simplicity, observed peaks at the pristine stage for the FE HZO will be referred as "double peak" or "double peak phenomenon" from now on. For positive voltages, the left peak shifts towards higher voltage values, whereas the right peak shifts towards lower voltage values, as shown by the red arrows. In terms of FE domains, this implies that certain FE domains are undergoing switching at lower voltage levels, while others are switching at higher values. With an increasing number of cycles, low-voltage switching domains transition to higher voltage values, while high-voltage switching domains transition to lower values, eventually resulting in the merging of the two peaks. In FE HZO thin films grown by sputtering, this effect has been already well described[30,31].

Although WU effect is rarely mentioned for AFE, we observed similar current peak displacement for ZrO_2 than for FE HZO as highlighted by the red arrows on figure 3(a) and (b). In contrast to FE HZO, the pristine values for AFE ZrO_2 exhibit different signs. It has to be mentioned that P_r doesn't apply for AFE, since around zero volt AFE are showing the same behavior as LD. Nevertheless, on figure 3(d), the two hysteresis loops of the AFE PE curves have smaller coercive fields and a higher P_s between pristine and woken states, leading to an increase in the ESD on Figure 4(a) as P_s increases and loss decreases.

This intriguing similarity between the double peak phenomenon in FE and the AFE behavior has already been discussed[11]. The non-uniform distribution of the internal electric field is likely attributed to unevenly distributed charged defects, such as oxygen vacancies, particularly near the electrodes. This asymmetry in oxygen vacancy concentration, often induced by the reduction of the doped HfO_2 layer by metal nitride electrodes, is a potential source of the internal field in the pristine material. The non-uniform distribution of oxygen vacancies near the electrodes may create an asymmetric internal field. In the process of electric field cycling, oxygen vacancies might diffuse into the bulk regions of fluorite-based films, triggering the wake-up process and resulting in the merging of switching current peaks in the case of FE HZO. Subsequent investigations have reported a redistribution of charges associated with oxygen vacancies[32,33]. Another plausible mechanism for the wake-up effect involves field-cycling-induced phase transitions[34]. Lomenzo et al.[12] initially proposed that the transition from the tetragonal (t-) to the ferroelectric orthorhombic phase (o-phase)

underlies the wake-up effect. They observed a decrease in dielectric permittivity and an increase in P_r with an increasing number of electric field cycles, possibly indicating a phase transition from a non-ferroelectric phase with higher permittivity to a ferroelectric phase with lower permittivity. Additionally, Grimley al. employed scanning transmission electron microscopy (STEM) and impedance spectroscopy to observe a phase transition from monoclinic (m-) to o-phase[35]. In essence, phase change and the redistribution of defects can induce the pinning of domains, leading to WU in both FE and AFE[36,37].

Despite the fact that some authors have considered that the double peak is not similar to AFE phenomena[11], the double peak on the positive voltage side can be considered as resulting from interactions between some negatively charged regions and positively charged regions or screened regions that define the switching current at the pristine stage. And after cycling, domains tend to homogenize, similarly to the observed phenomena for both FE HZO and AFE ZrO_2. Further investigations on the microstructure and oxygen vacancies re-organization would help to clearly determine if both phenomena have the same origin or not.

FE and AFE can reach high polarization values for low applied electric fields compared to dielectrics. This material functional property can be tailored for embedded energy storage capacitors of nanometer size that can reach high current density storage with low losses for low applied electric field. The electrical storage can be assessed on the thin film capacitor by calculating the energy storage density. By definition, the total energy W stored in a capacitor (expressed in joules) is the total work done in establishing the electric field from an uncharged state[38] :

$$W = \int_0^Q V(q)dq \tag{1}$$

By considering geometry factors in our Metal/Insulator/Metal (MIM) capacitors: the thickness of the insulator and the surface of the electrodes, it leads to the following expression of that the energy-storage density (ESD):

$$W_{ESD} = \int_0^{E_{max}} PdE \text{ (upon discharging)} \tag{2}$$

where it is considered that ESD is equal to W_{ESD}. As previously said, the definition for the total energy stored in equation 1 is calculated upon charging, starting from an uncharged

state, while ESD is calculated upon discharging, because the definition considers a perfect linear dielectric and therefore it does not take the losses (due to leakage current in the case of a LD) into account. Then, the loss can be calculated as :

$$W_{loss} = \int_0^{E_{max}} PdE \text{ (upon charging)} - W_{ESD} \tag{3}$$

As a consequence the efficiency (in percentage) of the charge/discharge is given by:

$$\eta = \frac{W_{ESD}}{W_{ESD} + W_{loss}} \times 100 \tag{4}$$

These calculations for ESD, loss and η are now standard performance indicator for fluorite-based capacitors.[13,39].

Figure 4 shows the ESD and η as a function of the number of cycles for an applied field of 3.5 MV/cm on the four analyzed samples and also for ZrO_2 cycled at 4 MV/cm. Contrary to the HZO FE layer, the breakdown field of the ZrO_2 AFE layer is higher allowing to display the film properties at 4 MV/cm. As expected, on Figure 4(a) one can observe the very high energy density of AFE ZrO_2 compared to the other samples. For LD HZO and ZrO_2, ESD is very low due to the low values of polarization when applying an electric field. But the samples have better endurance properties as they are not experiencing breakdown at 10^7 cycles, contrary to FE HZO and AFE ZrO_2. For FE HZO, at the early stage of cycling, the capacitor is very similar to AFE ZrO_2, because of the double peak phenomena. But as the number of cycles increases, switching peaks start to merge and ESD is therefore increasing, leading to a higher ESD for FE HZO than the one of AFE ZrO_2 at 10^3 cycles.

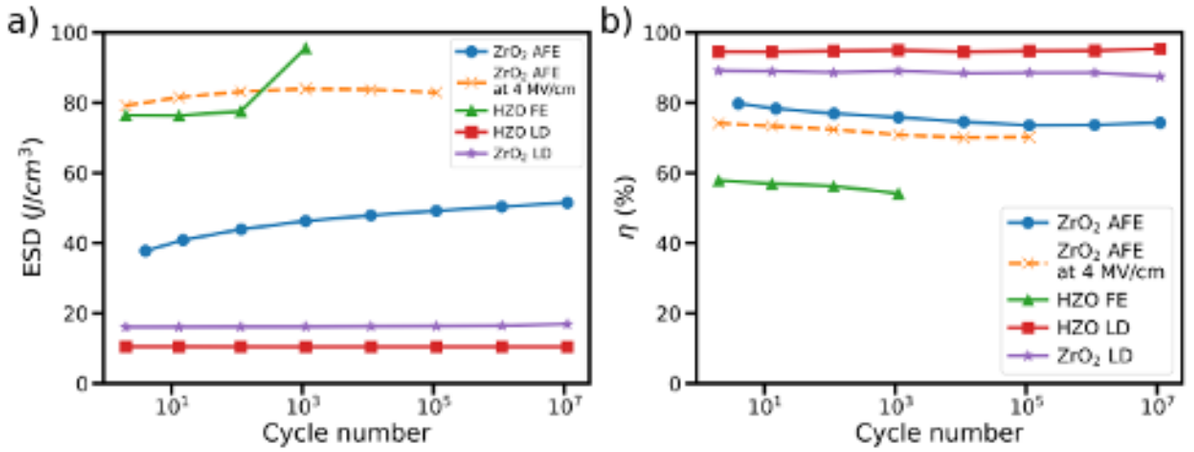

Figure 4. (a) Energy density storage versus cycles and (b) efficiency (η) versus cycles until breakdown for FE HZO, AFE ZrO_2, LD HZO and LD ZrO_2 at an applied electric field of 3.5 MV/cm. For comparison, AFE ZrO_2 at 4 MV/cm is also shown.

On Figure 4(b) as one could expect the most efficient samples are the LD ones. One can observe that η is actually not totally equal to 100 %, because of leakage currents and have the lowest ESD of all samples. As the hysteresis of FE HZO is wide opened, it has the highest losses, hence it shows the lowest η of the four samples of ≈ 55 %. At the same time, the high P_s of the FE sample make it reach the highest ESD value at 95 J/cm^3. Finally, the reason why AFE are considered as a better option for supercapacitors compared to simple FE and LD inorganic electrostatic capacitors, is because of their efficiency falling in between FE and LD, with an η of 75 % while their ESD is almost as high as the one of FE samples, reaching 52 J/cm^3 at 3.5 MV/cm. This value can be further increased up to 84 J/cm^3 at a higher electrical field (4.0 MV/cm).

The current literature for nanosupercapacitors using FE, AFE but also relaxor-ferroelectric (RFE) hafnium- and zirconium-based fluorite materials is compared with our results in Figure 5. One can observe that only few papers are showing higher ESD and η than our present work. Moreover, FE HZO is also showing excellent properties for nanosupercapacitor applications compared to what was previously observed for similar FE materials.

A limiting factor to further improve the ESD and efficiency in thin films is the FE and AFE film thickness scaling. Fluorite films have limited energy storage scaling properties due to the increase of the monoclinic phase proportion at large thicknesses[18]. However, the ESD

achieved for a thin film can be significantly enhanced by transitioning to a multilayered and three-dimensional (3D) structure[15], an aspect that can be explored in future studies. This transition holds the potential to elevate the ESD by several orders of magnitude, promising new avenues for enhanced energy storage capabilities. Investigations into the multilayered and 3D architectures thus represent an exciting frontier in the quest for optimizing energy storage efficiency, offering prospects for groundbreaking advancements in the field.

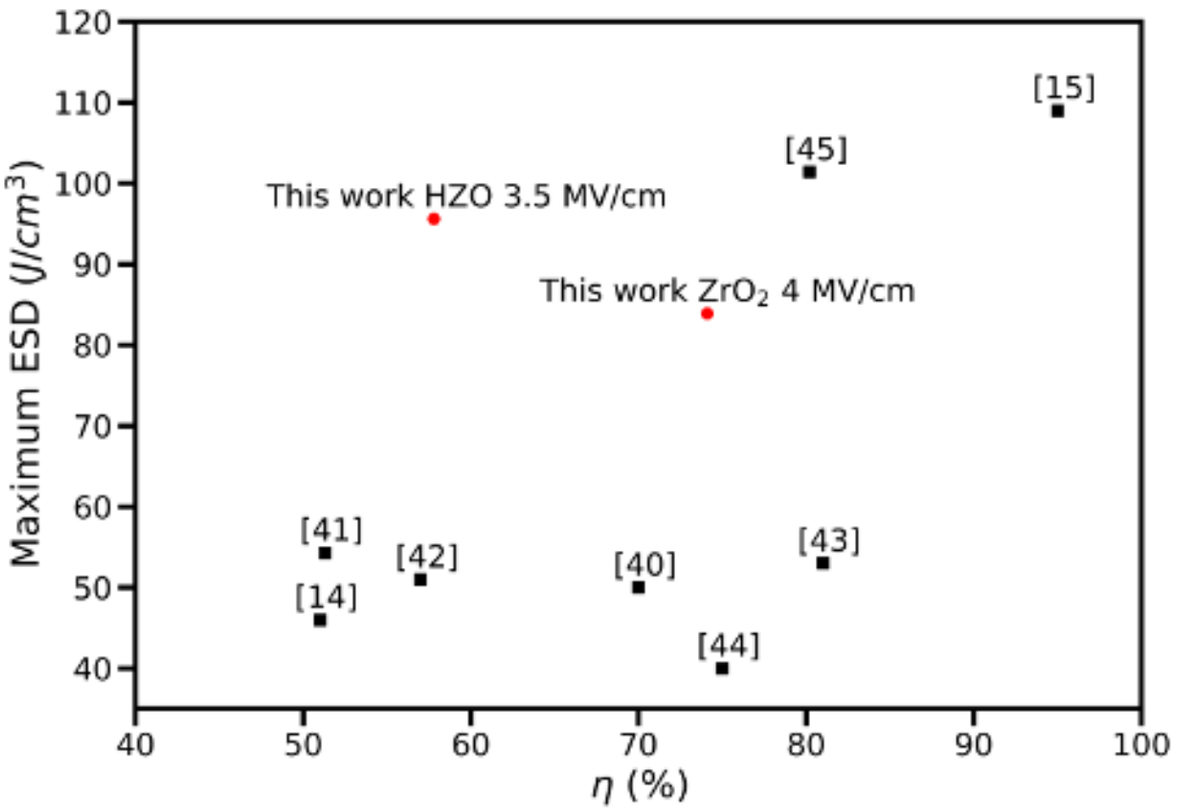

Figure 5. Comparison of FE and AFE properties of different fluorite nanosupercapacitors with a functional film thickness ranging from 5 to 15 nm from literature[14,15,40–45] (black squares) and our work (red circles).

IV. CONCLUSION

We investigated the potential of ferroelectric (FE) and antiferroelectric (AFE) fluorite-structured materials, such as hafnium oxide (HfO_2) and zirconium oxide (ZrO_2), for energy-efficient applications, addressing the urgent need to curb the soaring energy demands of the

digital age. By integrating these materials into existing CMOS technology, it demonstrates a forward-looking approach to enhancing electronic device efficiency through advanced energy conversion mechanisms. The research provides a comprehensive analysis of the structural and electrical properties of HZO and ZrO_2 thin films, showcasing their significant potential in solid-state electrostatic energy storage.

Moreover, the study compares the energy storage performances of FE, AFE, and LD samples, underlining the superior energy storage density (ESD) and efficiency of AFE materials. This finding is critical, as it highlights the promise of AFE ZrO_2 in energy storage applications, offering a balanced trade-off between high ESD and efficiency. The meticulous methodology, from synthesis to characterization, provides a robust framework for assessing the capabilities of these materials and sets a benchmark for future studies in the field.

SUPPLEMENTARY MATERIALS

See the supplementary material for an explanation of the applied electric field in the capacitors and polarization plots in function of the applied electric field at each measured cycles on all capacitors.

ACKNOWLEDGMENTS

This work was carried out on the NanoLyon technology platform and implemented inside the NanOx4EStor project. We would like to specifically thank Céline Chevalier, Giovanni Alaimo-Galli and Jean-Charles Roux for their implication on the research project at the NanoLyon platform. This NanOx4EStor project has received funding under the Joint Call 2021 of the M-ERA.NET3, an ERA-NET Cofund supported by the European Union's Horizon 2020 research and innovation program under grant agreement No 958174. This work was supported by the Portuguese Foundation for Science and Technology (FCT) in the framework of the M-ERA.NET NanOx4EStor Contract no. M-ERA-NET3/0003/2021, by Executive Agency for Higher Education, Research, Development and Innovation Funding (UEFISCDI) and by the Agence Nationale de la Recherche (ANR) under the contract ANR-22-MER3-0004-01.

AUTHOR DECLARATIONS

Conflict of Interest

The authors have no conflicts to disclose.

Data availability

The data that support the findings of this study are available from the corresponding author upon reasonable request.

REFERENCES

[1] "Digitalisation and energy," Tech. Rep. (International Energy Agency (IEA), 2017).

[2] J. P. B. Silva, K. C. Sekhar, H. Pan, J. L. MacManus-Driscoll, and M. Pereira, "Advances in dielectric thin films for energy storage applications, revealing the promise of group iv binary oxides," ACS Energy Letters **6**, 2208–2217 (2021).

[3] K. Mistry, C. Allen, C. Auth, B. Beattie, D. Bergstrom, M. Bost, M. Brazier, M. Buehler, A. Cappellani, R. Chau, *et al.*, "A 45nm logic technology with high-k+ metal gate transistors, strained silicon, 9 cu interconnect layers, 193nm dry patterning, and 100% pb-free packaging," in *2007 IEEE International Electron Devices Meeting* (IEEE, 2007) pp. 247–250.

[4] D. James, "Recent advances in memory technology," in *ASMC 2013 SEMI Advanced Semiconductor Manufacturing Conference* (IEEE, 2013) pp. 386–395.

[5] T. Böscke, J. Müller, D. Bräuhaus, U. Schröder, and U. Böttger, "Ferroelectricity in hafnium oxide thin films," Applied Physics Letters **99** (2011).

[6] T. Boescke, J. Heitmann, and U. Schroder, "Integrated circuit with dielectric layer," (2010), uS Patent 7,709,359.

[7] J. Müller, T. Böscke, D. Bräuhaus, U. Schröder, U. Böttger, J. Sundqvist, P. Kücher, T. Mikolajick, and L. Frey, "Ferroelectric zr0. 5hf0. 5o2 thin films for nonvolatile memory applications," Applied Physics Letters **99** (2011).

[8] J. Wang, H. Li, and R. Stevens, "Hafnia and hafnia-toughened ceramics," Journal of materials science **27**, 5397–5430 (1992).

[9]M. H. Park, Y. H. Lee, H. J. Kim, Y. J. Kim, T. Moon, K. D. Kim, J. Mueller, A. Kersch, U. Schroeder, T. Mikolajick, *et al.*, "Ferroelectricity and antiferroelectricity of doped thin hfo2-based films," Advanced Materials **27**, 1811–1831 (2015).

[10]X. Li, H. Zhong, T. Lin, F. Meng, A. Gao, Z. Liu, D. Su, K. Jin, C. Ge, Q. Zhang, and L. Gu, "Polarization switching and correlated phase transitions in fluorite-structure zro2 nanocrystals," Advanced Materials **35**, 2207736 (2023), https://onlinelibrary.wiley.com/doi/pdf/10.1002/adma.202207736.

[11]P. D. Lomenzo, L. Collins, R. Ganser, B. Xu, R. Guido, A. Gruverman, A. Kersch, T. Mikolajick, and U. Schroeder, "Discovery of nanoscale electric field-induced phase transitions in zro2," Advanced Functional Materials **33**, 2303636 (2023).

[12]P. D. Lomenzo, M. Materano, T. Mittmann, P. Buragohain, A. Gruverman, T. Kiguchi, T. Mikolajick, and U. Schroeder, "Harnessing phase transitions in antiferroelectric zro2 using the size effect," Advanced Electronic Materials **8**, 2100556 (2022).

[13]X. Hao, "A review on the dielectric materials for high energy-storage application," Journal of Advanced Dielectrics **3**, 1330001 (2013).

[14]M. H. Park, H. J. Kim, Y. J. Kim, T. Moon, K. D. Kim, and C. S. Hwang, "Thin hfxzr1-xo2 films: a new lead-free system for electrostatic supercapacitors with large energy storage density and robust thermal stability," Advanced Energy Materials **4**, 1400610 (2014).

[15]M. Hoffmann, F. P. G. Fengler, B. Max, U. Schroeder, S. Slesazeck, and T. Mikolajick, "Negative capacitance for electrostatic supercapacitors," Advanced Energy Materials **9**, 1901154 (2019).

[16]H. Chen, L. Liu, Z. Yan, X. Yuan, H. Luo, and D. Zhang, "Ultrahigh energy storage density in superparaelectric-like hf0.2zr0.8o2 electrostatic supercapacitors," Advanced Science **10**, 2300792 (2023).

[17]D. Zhou, J. Xu, Q. Li, Y. Guan, F. Cao, X. Dong, J. Müller, T. Schenk, and U. Schröder, "Wake-up effects in si-doped hafnium oxide ferroelectric thin films," Applied Physics Letters **103** (2013).

[18]M. Hyuk Park, H. Joon Kim, Y. Jin Kim, W. Lee, T. Moon, and C. Seong Hwang, "Evolution of phases and ferroelectric properties of thin hf0. 5zr0. 5o2 films according to the thickness and annealing temperature," Applied Physics Letters **102** (2013).

[19]H. Qi, A. Xie, and R. Zuo, "Local structure engineered lead-free ferroic dielectrics for superior energy-storage capacitors: A review," Energy Storage Materials **45**, 541–567 (2022).

[20]R. Materlik, C. Künneth, and A. Kersch, "The origin of ferroelectricity in hf1- xzrxo2: A computational investigation and a surface energy model," Journal of Applied Physics **117** (2015).

[21]G. Segantini, B. Manchon, I. Cañero Infante, M. Bugnet, R. Barhoumi, S. Nirantar, E. Mayes, P. Rojo Romeo, N. Blanchard, D. Deleruyelle, *et al.*, "Interplay between strain and defects at the interfaces of ultra-thin hf0. 5zr0. 5o2-based ferroelectric capacitors," Advanced Electronic Materials **9**, 2300171 (2023).

[22]J. Bouaziz, P. Rojo Romeo, N. Baboux, R. Negrea, L. Pintilie, and B. Vilquin, "Dramatic impact of pressure and annealing temperature on the properties of sputtered ferroelectric hzo layers," APL Materials **7** (2019).

[23]M. Hoffmann, Z. Wang, N. Tasneem, A. Zubair, P. V. Ravindran, M. Tian, A. A. Gaskell, D. Triyoso, S. Consiglio, K. Tapily, *et al.*, "Antiferroelectric negative capacitance from a structural phase transition in zirconia," Nature communications **13**, 1228 (2022).

[24]M. H. Park, Y. H. Lee, T. Mikolajick, U. Schroeder, and C. S. Hwang, "Review and perspective on ferroelectric hfo2-based thin films for memory applications," Mrs Communications **8**, 795–808 (2018).

[25]J. Bouaziz, P. Rojo Romeo, N. Baboux, and B. Vilquin, "Characterization of ferroelectric hafnium/zirconium oxide solid solutions deposited by reactive magnetron sputtering," Journal of Vacuum Science & Technology B **37** (2019).

[26]R. Cervasio, E. Amzallag, M. Verseils, P. Hemme, J.-B. Brubach, I. C. Infante, G. Segantini, P. Rojo Romeo, A. Coati, A. Vlad, *et al.*, "Quantification of crystalline phases in hf0. 5zr0. 5o2 thin films through complementary infrared spectroscopy and ab initio supercell simulations," ACS Applied Materials & Interfaces **16**, 3829–3840 (2024).

[27]C. Sim, Z. Zhou, X. Gao, H. Soon, and J. Wang, "Ferroelectric and fatigue behavior of pb (zr0. 52ti0. 48) o3/(bi3. 15nd0. 85) ti3o12 bilayered thin films," Journal of Applied Physics **103** (2008).

[28]J. Wu, J. Wang, D. Xiao, and J. Zhu, "Compositionally graded bismuth ferrite thin films," Journal of alloys and compounds **509**, L319–L323 (2011).

[29]S. Mueller, J. Muller, U. Schroeder, and T. Mikolajick, "Reliability characteristics of ferroelectric Si:HfO_2 thin films for memory applications," IEEE Transactions on Device and Materials Reliability **13**, 93–97 (2012).

[30]J. Bouaziz, P. R. Romeo, N. Baboux, and B. Vilquin, "Huge reduction of the wake-up effect in ferroelectric hzo thin films," ACS Applied Electronic Materials **1**, 1740–1745 (2019).

[31]B. Manchon, G. Segantini, N. Baboux, P. Rojo Romeo, R. Barhoumi, I. C. Infante, F. Alibart, D. Drouin, B. Vilquin, and D. Deleruyelle, "Insertion of an ultrathin interfacial aluminum layer for the realization of a hf 0.5 zr 0.5 o 2 ferroelectric tunnel junction," physica status solidi (RRL)–Rapid Research Letters **16**, 2100585 (2022).

[32]M. Pešić, F. P. G. Fengler, L. Larcher, A. Padovani, T. Schenk, E. D. Grimley, X. Sang, J. M. LeBeau, S. Slesazeck, U. Schroeder, *et al.*, "Physical mechanisms behind the field-cycling behavior of hfo2-based ferroelectric capacitors," Advanced Functional Materials **26**, 4601–4612 (2016).

[33]W. Hamouda, F. Mehmood, T. Mikolajick, U. Schroeder, T. O. Mentes, A. Locatelli, and N. Barrett, "Oxygen vacancy concentration as a function of cycling and polarization state in TiN/Hf0.5Zr0.5O2/TiN ferroelectric capacitors studied by x-ray photoemission electron microscopy," Applied Physics Letters **120**, 202902 (2022).

[34]H. J. Kim, M. H. Park, Y. J. Kim, Y. H. Lee, T. Moon, K. Do Kim, S. D. Hyun, and C. S. Hwang, "A study on the wake-up effect of ferroelectric hf 0.5 zr 0.5 o 2 films by pulse-switching measurement," Nanoscale **8**, 1383–1389 (2016).

[35]E. D. Grimley, T. Schenk, X. Sang, M. Pešić, U. Schroeder, T. Mikolajick, and J. M. LeBeau, "Structural changes underlying field-cycling phenomena in ferroelectric hfo2 thin films," Advanced Electronic Materials **2**, 1600173 (2016).

[36]F. P. Fengler, M. Pešić, S. Starschich, T. Schneller, C. Künneth, U. Böttger, H. Mulaosmanovic, T. Schenk, M. H. Park, R. Nigon, *et al.*, "Domain pinning: Comparison of hafnia and pzt based ferroelectrics," Advanced Electronic Materials **3**, 1600505 (2017).

[37]F. Fengler, M. Hoffmann, S. Slesazeck, T. Mikolajick, and U. Schroeder, "On the relationship between field cycling and imprint in ferroelectric hf0. 5zr0. 5o2," Journal of Applied Physics **123** (2018).

[38]E. M. Purcell and D. J. Morin, *Electricity and Magnetism*, 3rd ed. (Cambridge University Press, 2013).

[39]S.-H. Yi, H.-C. Lin, and M.-J. Chen, "Ultra-high energy storage density and scale-up of antiferroelectric tio2/zro2/tio2 stacks for supercapacitors," J. Mater. Chem. A **9**, 9081–9091 (2021).

[40]M. G. Kozodaev, A. G. Chernikova, R. R. Khakimov, M. H. Park, A. M. Markeev, and C. S. Hwang, "La-doped hf0. 5zr0. 5o2 thin films for high-efficiency electrostatic supercapacitors," Applied Physics Letters **113** (2018).

[41]J. P. B. Silva, J. Silva, K. Sekhar, H. Palneedi, M. Istrate, R. Negrea, C. Ghica, A. Chahboun, M. Pereira, and M. Gomes, "Energy storage performance of ferroelectric zro 2 film capacitors: effect of hfo 2: Al 2 o 3 dielectric insert layer," Journal of Materials Chemistry A **8**, 14171–14177 (2020).

[42]K. Do Kim, Y. H. Lee, T. Gwon, Y. J. Kim, H. J. Kim, T. Moon, S. D. Hyun, H. W. Park, M. H. Park, and C. S. Hwang, "Scale-up and optimization of hfo2-zro2 solid solution thin films for the electrostatic supercapacitors," Nano Energy **39**, 390–399 (2017).

[43]P. D. Lomenzo, C.-C. Chung, C. Zhou, J. L. Jones, and T. Nishida, "Doped Hf0.5Zr0.5O2 for high efficiency integrated supercapacitors," Applied Physics Letters **110**, 232904 (2017).

[44]K. Kühnel, M. Czernohorsky, C. Mart, and W. Weinreich, "High-density energy storage in Si-doped hafnium oxide thin films on area-enhanced substrates," Journal of Vacuum Science & Technology B **37**, 021401 (2019).

[45]W. Shuai, J.-Y. Dai, Z. Xu, G. Tian, C. Luo, M. Li, R. Tao, Z. Fan, D. Chen, G. Zhou, X. Lu, and J. Liu, "Superior and ultrafast energy storage performance of relaxorantiferroelectric hfo2-based supercapacitors," Energy Storage Materials **62**, 102931 (2023).